SCIENTIFIC REPORTS

OPEN

SUBJECT AREAS:
ION CHANNEL SIGNALLING
NEUROSCIENCE
MOLECULAR NEUROSCIENCE
SYNAPTIC VESICLE EXOCYTOSIS

Received
7 February 2013

Accepted
26 March 2013

Published
9 April 2013

Correspondence and requests for materials should be addressed to D.A. (datlas@vms.huji.ac.il)

* These authors contributed equally to this work.

Intra-membrane Signaling Between the Voltage-Gated Ca^{2+}-Channel and Cysteine Residues of Syntaxin 1A Coordinates Synchronous Release

Niv Bachnoff*, Moshe Cohen-Kutner*, Michael Trus & Daphne Atlas

The Hebrew University of Jerusalem, Institute of Life Sciences, Dept. of Biological Chemistry, Givat-Ram, Jerusalem, 91904, Israel.

The interaction of syntaxin 1A (Sx1A) with voltage-gated calcium channels (VGCC) is required for depolarization-evoked release. However, it is unclear how the signal is transferred from the channel to the exocytotic machinery and whether assembly of Sx1A and the calcium channel is conformationally linked to triggering synchronous release. Here we demonstrate that depolarization-evoked catecholamine release was decreased in chromaffin cells infected with semliki forest viral vectors encoding Sx1A mutants, $Sx1A^{C271V}$, or $Sx1A^{C272V}$, or by direct oxidation of these Sx1A transmembrane (TM) cysteine residues. Mutating or oxidizing these highly conserved Sx1A Cys271 and Cys272 equally disrupted the Sx1A interaction with the channel. The results highlight the functional link between the VGCC and the exocytotic machinery, and attribute the redox sensitivity of the release process to the Sx1A TM C271 and C272. This unique intra-membrane signal-transduction pathway enables fast signaling, and triggers synchronous release by conformational-coupling of the channel with Sx1A.

Voltage-driven conformational changes open the pore of voltage-gated Ca^{2+} channels (VGCC) to facilitate Ca^{2+}-binding at the pore followed by Ca^{2+} permeation into the cell. A signal initiated by the conformational coupling between voltage-sensing domains and a Ca^{2+}-occupied channel pore has been proposed to trigger exocytosis prior to Ca^{2+} influx (review[1,2]). The signal is presumed to propagate from the channel pore positioned at the membrane bilayer to the transmembrane (TM) domain of syntaxin 1A (Sx1A), the only exocytotic SNARE protein harboring a cellular TM segment. Sx1A physically associates with VGCC channel via the cytosolic II–III domain of the VGCC[3,4]. Functionally, Sx1A modifies current amplitude and the activation kinetics of Cav1.2[5], Cav2.2[6,7,4], Cav2.3[8], and Cav2.1[9–13]. Replacing of Sx1A TM domain with the Sx2 TM domain obliterates Sx1A interaction with the channel, revealing an interacting interface between the TM domain of Sx1A and the channel[14]. The bidirectional Sx1A/channel cross talk through Sx1A TM interface negatively modulates current amplitude, while molecular determinants of the Sx1A cytosolic domain modify the activation kinetics of the channels[1,2,5,14–16]. Two highly conserved Cys271 and C272 residues within the Sx1A TM segment are essential for Sx1A interaction with the channel[14,16]. A simulated secretory system was created by injection of the recombinant channel subunits plus Sx1A, SNAP-25, and synaptotagmin into *Xenopus* oocytes, and secretion was measured by means of capacitance increase. The assembly of the channel with Sx1A, SNAP-25, and synaptotagmin generated an exocytotic unit called excitosome, in which the channel kinetics differ from wild type channel[17,4,18]. In this reconstituted system replacement of Sx1A C271 or C272 obliterated a capacitance jump triggered by membrane depolarization[19,20].

The rate of secretion, ~200 μsec, is within the time span of conformational changes. It led us to suggest that the fusion of vesicles tethered to the membrane via a primed excitosome-complex, is a conformational-triggered event[21,22,2,11]. A coupling between the calcium channel and the exocytotic machinery during channel pore opening could impart a fast signal transduction essential for triggering synchronous transmitter release.

In the present study we used a combination of biochemical, chemical, and physiological approaches to characterize the role of Sx1A in transmitting the exocytotic signal. The functional aspects of this mechanism were evaluated using amperometry in a physiological secretory system, the bovine chromaffin cells, and voltage-clamped recordings using the *Xenopus* oocytes expression system. In dominant-negative experiments, the Sx1A mutants $Sx1A^{C271V}$, $Sx1A^{C272V}$ and $Sx1A^{C271V/C272V}$ ($Sx1A^{CC/VV}$) were introduced into chromaffin cells by viral

infection, causing a profound inhibition of depolarization-evoked CA release. Similarly, direct oxidation of the highly conserved C271 and C272 abolished CA release. These results strongly correlate with voltage-clamp *Xenopus* oocytes studies, in which the contact of Sx1A with the channel is lost either by mutating or oxidizing C271 and C272. Our results support the model in which Sx1A transduces a signal from the channel to promote fast signaling of secretion[21,22,11]. Propagation of this signal through the Sx1A TM domain to trigger secretion is consistent with our excitosome model[17,18]. This model proposes that a conformational coupling during channel activation triggers transmitter release in sub-milliseconds by a unique intra-membrane signaling pathway prior to Ca^{2+}-entry.

Results

Sx1A$^{CC/VV}$ down-regulates depolarization-evoked release in bovine chromaffin cells. In a previous study electrical stimulation of *Xenopus* oocytes co-expressing Sx1A, SNAP-25, synaptotagmin and VGCC, triggered a capacitance change, which was lost when the Sx1A mutants were expressed instead of Sx1A[20]. To evaluate these reconstitution results using a physiological secretory system, we tested the loss of fast synchronous release in chromaffin medullary cells. We performed dominant negative experiments using Semliki Forest viral expression vectors (pSPV) to express the Sx1A mutants: Sx1A^{C271V}, Sx1A^{C272V}, Sx1A$^{C271V/C272V}$ (Sx1A$^{CC/VV}$), or Sx1A^{C145A}. The construct pSFV wt Sx1A served as a positive control. The SFV infection system itself, was highly efficient showing ~ 90% infection rate. Membrane targeting of RFP-wt Sx1A and RFP-Sx1A$^{CC/VV}$ was shown by confocal microscopy (**Fig. 1a**). The expressed proteins were densely localized to the cell membrane and absent in non-infected cells, or in cells infected with GFP only (**Fig. 1a**). Using western blot analysis, the protein level of RFP-wt Sx1A, and Sx1A mutant (59kD), as well as endogenous Sx1A (33kD) was quantified. The protein levels of RFP-wt Sx1A and Sx1A mutants were similar and comparable to that of endogenous Sx1A (**Fig. 1b, c**).

CA release was triggered by membrane depolarization in cells infected with one of the Sx1A mutants and monitored by amperometry[23,22]. Amperometric current, which is seen as a spike when a fusion pore opens, represents CA released from a single vesicle with 2.5 ms rise-time. Therefore, the amperometry events represent a relatively early kinetic step in the process of secretion[24].

Release was triggered using a puff of 60 mM KCl (K60) for 10 sec, in control cells, GFP-infected cells, or cells infected with RFP-wt Sx1A or RFP-Sx1A$^{CC/VV}$, as shown by the amperometry spikes in exemplary cells (**Fig. 2a**). The release of individual secretory events was monitored over one min. We measured the frequency of CA release, which reflects the actual opening of fusion pores, the number of spikes per cell, and the total amount of secretion taken from the average area under the spikes. The overall time course of secretion was determined from normalized waiting time distributions constructed by spike counting. The infection itself slightly reduced the number of spikes compared to control non-infected cells, from 27.7 ± 2.4 spike/cell (n = 21) to 22.5 ± 3.1 spike/cell (n = 32) in GFP-infected cells (**Table I**). Cells infected with RFP wt Sx1A showed a similar cumulative number of events, 22.8 ± 2.4 spike/cell; (n = 23) to GFP infected cells. In contrast, a significantly lower secretion of ~ 50%, was observed in the RFP-Sx1A$^{CC/VV}$-infected cells (10.9 ± 0.8 spikes/cell; n = 32) (**Fig. 2b**, ***left;*** **Fig. 2c** ***left)***. The net CA secretion during the initial 10–30 sec of the secretion was determined for individual cells and then averaged for each cell. It was 50% reduced from 11.5 ± 1.2 pC in wt Sx1A infected-cells to 6.0 ± 0.8 pC in Sx1A$^{CC/VV}$ infected-cells (**Fig. 2c** ***middle***; **Table I**). The maximal slopes of the corresponding cumulative spike plots were taken to represent the initial rates of secretion. The initial secretion rates were lower in cells infected with Sx1A$^{CC/VV}$ (0.40 ± 0.01 spikes/sec) compared to GFP (0.80 ± 0.04 spikes/sec), or wt Sx1A infected cells (0.71 ± 0.03 spikes/sec) (**Fig. 2b** ***right;*** **Fig. 2c** ***right***; **Table I**). These

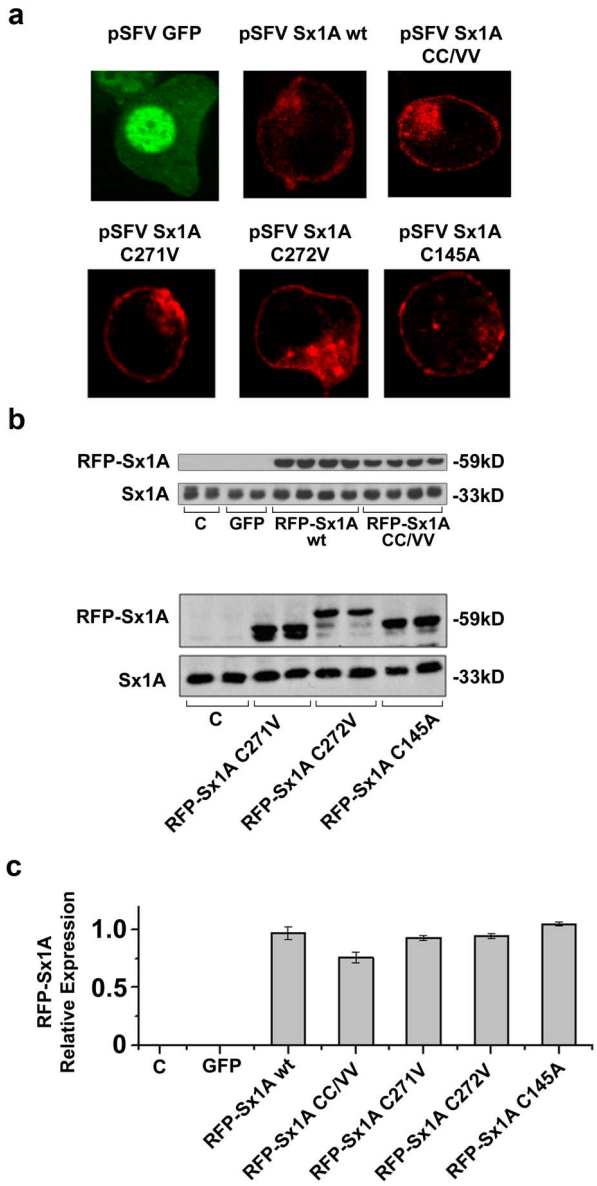

Figure 1 | Expressing GFP, wt Sx1A, and Sx1A mutant Sx1A^{C271V}, Sx1A^{C272V} and Sx1A^{C145A} by SFV vectors in bovine chromaffin cells. (a) Chromaffin cells were infected with SFV vectors of GFP, RFP-Sx1A wt, RFP-Sx1A$^{CC/VV}$, RFP-Sx1A^{C271V}, RFP-Sx1A^{C272V} and RFP-Sx1A^{C145A}. The cells were visualized by confocal microscopy (b) Western blot analysis of Sx1A expression was determined in cell lysates from chromaffin cells infected with SFV-GFP, RFP-wt Sx1A, RFP-Sx1A$^{CC/VV}$ (*upper*), RFP-Sx1A^{C271V} or RFP-Sx1A^{C272V} or RFP-Sx1A^{C145A} (*lower*) (c) Quantification of the relative expression of RFP-wtSx1A and RFP-Sx1A mutants to endogenous Sx1A present in the cells.

dominant-negative effects of Sx1A$^{CC/VV}$ on secretion are consistent with the results of capacitance changes monitored in a reconstituted oocyte system[20]. Moreover, the decrease in the initial rate of secretion implies that more than one Sx1A molecule interacts with the channel, further inferring that native and mutated Sx1A generate mixed clusters that are less efficient at triggering CA secretion, compared to clusters assembled by native Sx1A only.

Sx1A^{C271V} and Sx1A^{C272V} down-regulate depolarization-evoked release in bovine chromaffin cells. Next, we examined which of the two adjacent Cys residues C271 or C272 is essential for inhibiting secretion. Chromaffin cells were infected with pSFV

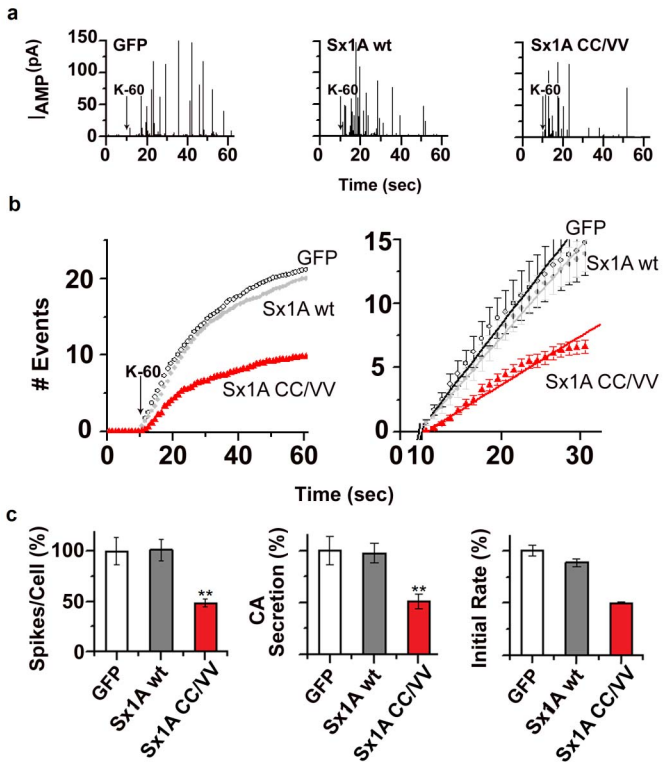

Figure 2 | Sx1A$^{CC/VV}$ mutant affects depolarization evoked secretion in bovine chromaffin cells. (a) Sample amperometry traces for control, GFP-infected, RFP wt Sx1A infected, and RFP-Sx1A$^{CC/VV}$ infected cells elicited by a puff of K60, indicated by the arrow (b) *Left*, Cumulative spike counts were plotted versus time to illustrate the time course of secretion triggered by depolarization (starting at t =10). *Right*, expanded view of the initial cumulative spike counts shown in b *left* (c) *Left*, average number of spikes per cell. *Middle*, The average area underneath the spikes represents the total mean charge (total CA secretion) and is presented as the percentage of average secretion per cell. *Right*, the mean frequency of the initial rate was calculated as the maximum slope in plot b *right*, during the first 30 sec of recording (Table II). $^{**}p < 0.005$.

encoding RFP-tagged wt Sx1A, -Sx1A^{C271V}, or -Sx1A^{C272V}. Membrane targeting of the RFP-Sx1A mutants was visualized by fluorescence using confocal microscopy (**Fig. 1a**). Both RFP-Sx1A^{C271V} and RFP-Sx1A^{C272V} mutants were densely localized at the cell membrane, similar to RFP-wt Sx1A, and were absent in non-infected or in GFP infected cells (**Fig. 1a**). The protein levels of RFP-wt Sx1A, RFP-Sx1A^{C271V}, RFP-Sx1A^{C272V} and RFP-Sx1A^{C145A} (59 kD) were not statistically different, and were comparable to the endogenous Sx1A (33 kD) level, as quantified by western blot analysis using anti-Sx1A antibodies (**Fig. 1b,c**).

CA release is shown in representative cells infected with Sx1A^{C271V}, Sx1A^{C272V}, or Sx1A^{C145A} (**Fig. 3a**) and in cumulative plots (**Fig. 3b**, ***left)***. The infection procedure alone reduced the number of spikes in non-infected cells from 35.7 ± 4 spike/cell (n = 13) to 25.1 ± 4.3 spike/cell (n = 9) in GFP-infected cells (**Table II**). A significantly smaller number of events were seen in Sx1A^{C271V} (10.9 ± 1.2 spike/cell; n = 14) and Sx1A^{C272V} (11.8 ± 1.6 spikes/cell: n = 13) infected cells, compared to GFP infected cells (25.1 ± 4.3 spike/cell; **Table II**). The mutations also affected the slope of the cumulative plots, which corresponds to the initial rate of secretion (**Fig 3b, *right;* Table II**; **Fig. 3c *right***). The release frequency calculated from the corresponding slopes was ~ 50% lower in Sx1A^{C271V} and Sx1A^{C272V} infected cells compared to GFP infected cells (**Fig 3c**, right; **Table II**). The considerable decrease in the initial rate caused by Sx1A^{C271V} or Sx1A^{C272V} was similar to the effect of Sx1A$^{CC/VV}$, implying a lower efficiency of the secretory process (**Fig. 3b *right*; Fig. 3c *middle*; Table II**). The results further support the view that native and mutated Sx1A might combine to form 'inefficient mixed clusters', in which signaling between the channel and Sx1A is disrupted, leading to inhibition of secretion.

Correspondingly, net CA released during the initial 30 sec was reduced by 45% in GFP infected-cells, from 14.3 ± 2.9 pC to 8.0 ± 1.3 pC in Sx1A^{C271V} infected-cells, or 50%, to 7.2 ± 1.1 in Sx1A^{C272V} infected-cells (**Fig. 3c, *middle*; Table II**).

As opposed to cells infected with Sx1A TM mutants, cells infected with Sx1A^{C145A}, in which the single cytosolic Cys was mutated, exhibited similar number of spikes (22.5 ± 1.9 spikes/cell; n = 22) and similar initial rate (7.8 ± 0.03 spikes/sec) to GFP-infected cells (**Fig. 3**), indicating no impact of the intracellular Cys145 on evoked-CA release in chromaffin cells. The kinetic parameters of each spike and pre-spike (foot parameters) calculated in cells infected with GFP, Sx1A or any of the four Sx1A mutants, displayed no significant differences (**Table SI** and **Table SII**).

The TM domain of Sx1A modulates VGCC kinetics. We next tested whether the dominant negative effects of Sx1A resulted from a direct interaction of C271 and C272 with VGCCs, Cav1.2 (L-type calcium channel), or Cav2.1 (P/Q type calcium channel). Both Cys residues were mutated to Ala, (Sx1A$^{CC/AA}$), Ser (Sx1A$^{CC/SS}$) or Val (Sx1A$^{CC/VV}$) (**Fig. 4a,b**) and the corresponding cRNAs of the RFP-tagged mutants were injected into *Xenopus* oocytes. The level of expression was visualized four days after injection by confocal imaging (**Fig. 4a**). Confocal images showed a similar fluorescence level distributed at the cell membrane for wt and Sx1A mutants (**Fig. 4a**). Also the protein levels of RFP wt Sx1A and the corresponding Sx1A mutants were similar and comparable to endogenous Sx1A, as shown by western blot analysis using anti Sx1A antibodies (**Fig. 4c**).

The molecular specificity of the Sx1A functional-interaction with the VGCC was examined in oocytes expressing both Sx1A and the channel using the standard two-electrode voltage-clamped assay. The three-channel subunits $\alpha_1$1.2 (L), α_2/δ, and β2A or $\alpha_1$2.1 (P/Q), α_2/δ, and β3, were injected in equimolar concentrations to oocytes as previously reported[5,11]. Twenty-four hrs later, cRNAs of the corresponding RFP-tagged Sx1A mutants, Sx1A$^{CC/SS}$, Sx1A$^{CC/AA}$, or Sx1A$^{CC/VV}$ were injected into the oocytes and inward currents were recorded five days after injection of the channel cRNA[17]. The effects

Table I | Spike number, initial rates, and total CA release induced by a 10 sec puff of K60 in bovine chromaffin cells infected with GFP, Sx1A wt, and Sx1A$^{CC/VV}$

	Cell (n)	Spikes (n)	Initial rate (Spikes/sec)	Initial secretion (pC)	Spikes/cell (n)	Spikes/cell (Inhibition) [a] (%)
Control	21	581	0.73 ± 0.03	14.6 ± 2.1	27.7 ± 2.4	-
pSFV **GFP**	32	721	0.80 ± 0.04	11.7 ± 1.6	22.5 ± 3.1	-
pSFV **Sx1A wt**	23	524	0.71 ± 0.03	11.5 ± 1.1	22.8 ± 2.4	0
pSFV **Sx1A$^{CC/VV}$**	32	350	0.40 ± 0.01	6.0 ± 0.8***	10.9 ± 0.8***	52

***p < 0.005
[a]Percent inhibition compared to GFP-infected cells.

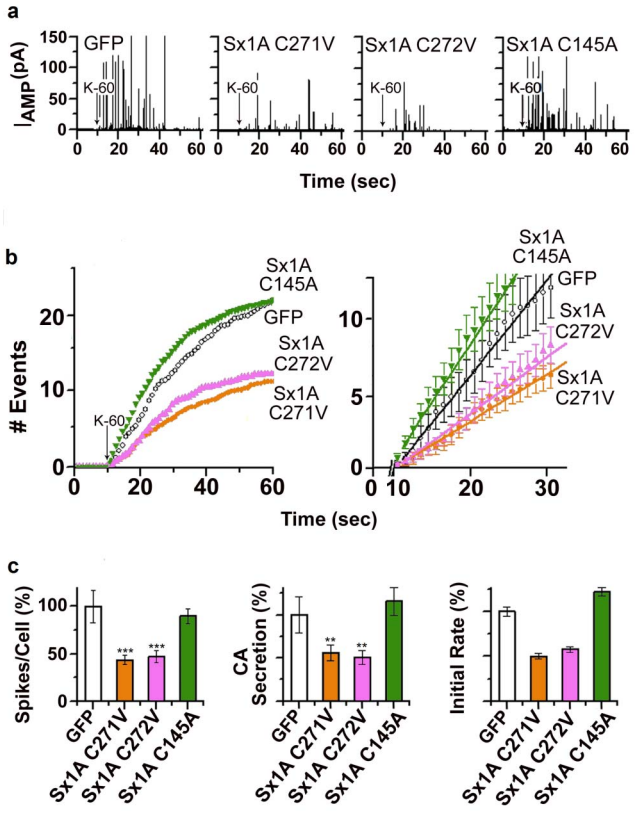

Figure 3 | Sx1A mutants Sx1A^{C271V}, and Sx1A^{C272V} affect secretion rate in bovine chromaffin cells. (a) Sample amperometry traces for GFP, and RFP-Sx1A^{C271V}, RFP-Sx1A^{C272V}, and RFP-Sx1A^{C145A} mutants elicited by a puff of K60 (arrow) (b) *Left*, Cumulative spike counts were plotted versus time to illustrate the time course of fusion triggered by depolarization (starting at t = 10). *Right*, expanded view of the initial cumulative spike counts. The mean frequency of the initial rate was calculated as the maximum slope in plot b *left* during the first 20 s of K60 stimulation (Table II) (c) *Left*, average number of spikes per cell (Table II), *Middle*, the average area underneath the spikes represents the total mean charge (total CA secretion) and is presented as the percentage of average secretion per cell. *Right*, the mean frequency of the initial rate was calculated as the maximum slope in plot b *right*, during the first 30s of recording. $^{**}p < 0.05$; $^{***}p < 0.005$.

of C271 and C272 substitution in Sx1A on Cav1.2 kinetics by the smaller residue Ala, the partially polarized Ser, or Val with no polarity, are shown in **Fig. 4d,e,f**. Both superimposed current traces elicited from a resting potential of −80 mV to +30 mV, and current-voltage relationship showed modulation of inward current by RFP Sx1A, as previously demonstrated[5]. In contrast, the current amplitude was hardly affected by the Sx1A mutants (**Table SIII; Fig. 4d,e**). The RFP-Sx1A and RFP-Sx1A$^{CC/AA}$ mutants showed no shift in the voltage-conductance plot, while RFP-Sx1A$^{CC/SS}$ and RFP-Sx1A$^{CC/VV}$ displayed a small shift to negative voltages, from 11.5 ± 0.8 to 6.8 ± 0.7 and 6.3 ± 1.4 mV, respectively (**Table SIII**; **Fig. 4f**).

Current amplitude of the neuronal P/Q-type channel (Cav2.1), similar to Cav1.2, was negatively modulated by RFP-Sx1A and hardly affected by the Sx1A mutants (**Fig. S1; Table SIII**).

The redox sensitivity of Sx1A/channel interaction. Inhibition of secretion by Sx1A mutants led us to explore the effects of oxidized C271 and C272 on signal transduction between the channel and Sx1A. Oocytes expressing the three-channel subunits $\alpha_1$1.2, $\alpha_2\delta$, and the β2A, with or without Sx1A, were exposed to the oxidizing reagent AuF, an organo-gold molecule, which is a linear two-coordinate complex that contains gold in the +1 oxidation, a triethylphosphine and tetra acetyl thioglucose, and is highly reactive towards thiol groups[25]. Inward currents were stimulated from a holding potential of −80 mV to various test potentials in 5 mV increments in response to a 200 ms test pulse, using the two-electrode voltage clamped standard assay[17] (**Fig. 5**). AuF applied at 5 μM for 30 min did not affect current amplitude and channel inactivation, as shown by the superimposed current traces elicited to +25 mV (**Fig. 5a *left*, 5b *left***). It also did not alter the voltage-conductance ratio, G/Gmax (**Fig. 5c *left***) but significantly increased the rate of Cav1.2 activation, as demonstrated by the voltage-dependent decrease in the time constant of activation (**Fig. 5d *left***). Treatment with AuF negated the inhibitory effect of Sx1A on current amplitude (2500 ± 150 to 1200 ± 140 nA) (**Fig. 5a *middle*, 5b *middle***), suspended the Sx1A-induced shift in conductivity (G/Gmax) towards positive voltages (**Fig. 5c *middle***), and increased the rate of activation (**Fig. 5d *middle***).

The addition of a reducing reagent, NAC-amide (AD4)[26,27] reversed the AuF effect on channel kinetics as monitored by current amplitude (**Fig. 5a *right*, 5b *right***), voltage conductivity (G/Gmax) (**Fig. 5c *right*),** and channel activation (**Fig. 5d**; ***right***). The redox sensitivity of Sx1A crosstalk with the channel, which was lost upon oxidation with AuF and resumed by reducing compounds, most likely reduced the free thiol groups of Sx1A, C271 and C272. In contrast, modulation of channel kinetics by the cytoplasmic Sx1A^{C145A} mutant was similar to wt Sx1A, confirming that the redox sensitivity of VGCC/Sx1A interaction was conferred by the TM Cys residues (**Fig. S2; Table SIII**).

The Biotin-Switch assay demonstrates AuF binding to Sx1A TM Cys residues. AuF exhibits a dual effect on chromaffin cells; it inhibits CA release in a time range of 25–30 min, and phosphorylates MAP kinases in 3–4 hrs[28]. These effects are likely to result either from a direct oxidizing effect on the exocytotic machinery, or from changes in the redox state of the cell, caused by selective inhibition of thioredoxin reductase by AuF, or both[29].

A biochemical approach was employed to explore whether the short-term effect of AuF on evoked release resulted from oxidizing a redox-sensitive protein of the exocytotic machinery. For that purpose the accessibility and ability of Sx1A to react with

Table II | Spike number, initial rates, and total release of CA induced by a 10 sec puff of K60 in bovine chromaffin cells infected with GFP, Sx1A wt, and either Sx1A^{C271V}, Sx1A^{C272V}, or Sx1A^{C145A}

	Cell (n)	Spikes (n)	Initial rate (Spikes/sec)	Initial secretion (pC)	Spikes/Cell (n)	Spikes/Cell (Inhibition) [a](%)
Control	13	464	0.77 ± 0.04	14.3 ± 1.9	35.7 ± 4.0	—
pSFV **GFP**	9	226	0.64 ± 0.03	14.3 ± 2.9	25.1 ± 4.3	—
pSFV **Sx1A^{C271V}**	14	153	0.32 ± 0.02	8.0 ± 1.3**	10.9 ± 1.2***	57
pSFV **Sx1A^{C272V}**	13	153	0.37 ± 0.02	7.2 ± 1.1**	11.8 ± 1.6***	53
pSFV **Sx1A^{C145A}**	22	496	0.78±0.03	16.6 ± 2.3	22.5 ± 1.9	11

$^{**}p < 0.05$; $^{***}p < 0.005$
[a]Percent inhibition compared to GFP-infected cells.

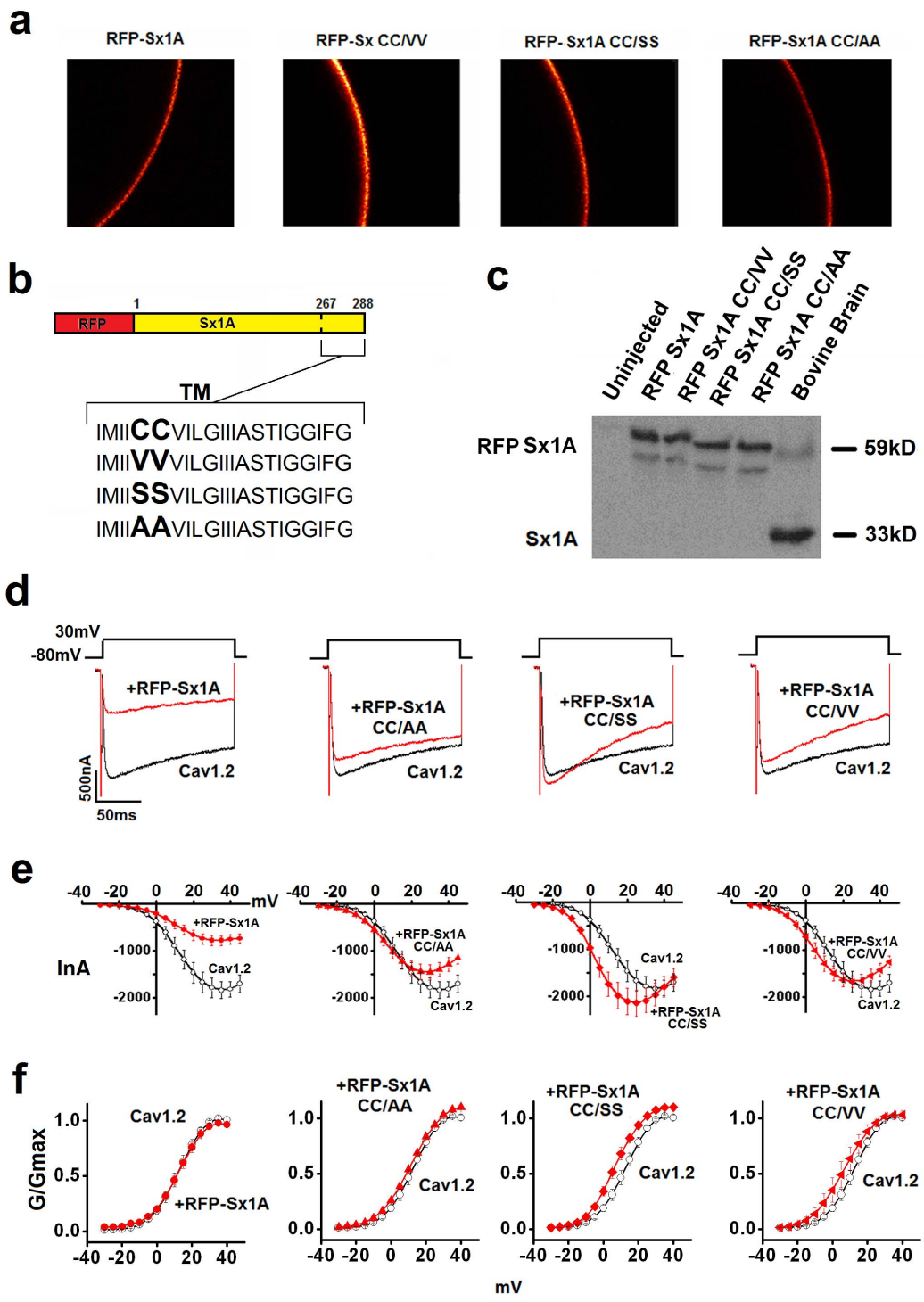

Figure 4 | Different mutations in C271, C272 of Sx1A are expressed and targeted to the membrane of *Xenopus* laevis oocytes affecting current flow through Cav1.2 channel. (a) Confocal images of oocytes expressing RFP-tagged wt Sx1A and RFP-tagged Sx1A$^{CC/VV}$, Sx1A$^{CC/SS}$, Sx1A$^{CC/AA}$ mutants (b) Schematic depiction of TMD location of the Sx1A Cys271, and Cys272 Sx1A residues (c) Western blot analysis of RFP-wt and RFP-Sx1A mutants expressed in *Xenopus* oocytes and a bovine brain sample, as indicated. Blots were incubated with anti-Sx1A antibody. (d) Representative superimposed $\alpha_1$1.2/β2/α2δ current traces (Cav1.2) in the absence and in the presence of RFP-Sx1A (*left*); RFP-Sx1A$^{CC/AA}$ (*middle-left*); RFP-Sx1A$^{CC/SS}$ (*middle-right*) and RFP-Sx1A$^{CC/VV}$ (*right*) (e) Leak subtracted current-voltage relationships of $\alpha_1$1.2/β2/α2δ expressed either alone (○) or with RFP-Sx1A (●, *left*); RFP-Sx1A$^{CC/AA}$ (▲, *middle-left*); RFP-Sx1A$^{CC/SS}$ (◆, *middle-right*); RFP-Sx1A$^{CC/VV}$ (◀, *right*). (f) Voltage-conductance (G/Gmax) analysis of $\alpha_1$1.2/β2/α2δ expressed either alone or with the different mutants, as indicated in B. The data points correspond to the mean ± SEM of currents (n = 12–14). Individual data points are mean ± SEM (n = 12–14). The results were fitted to the sigmoidal Boltzmann equation.

biotin-N-maleimide (biotin-NM), a specific probe that labels thiol groups, was tested using a modified Biotin-Switch assay[30], as schematically shown in **Fig. 6a**. Chromaffin cells (**Fig. 6b**) or oocytes (**Fig. 6c**) were exposed to 5 μM AuF followed by10 mM ascorbic acid and then incubated with 2 mM (biotin-NM). This was followed by affinity purification with strep-avidin beads and immunoblot analysis using Sx1A antibody. The lower levels of Sx1A pulled-down after treatment with AuF, indicate that oxidation by AuF prevented

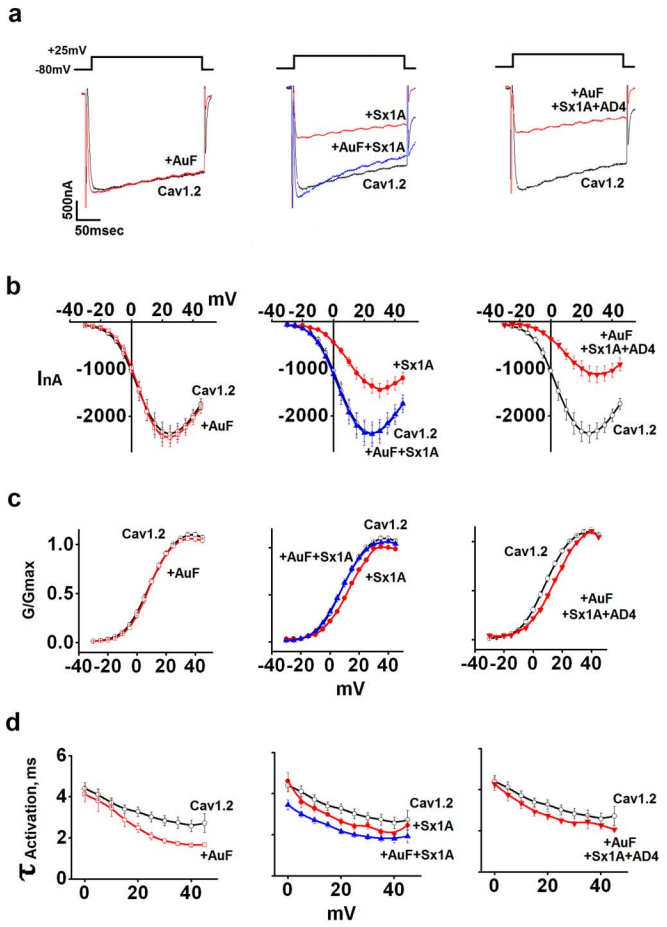

Figure 5 | The interaction between Sx1A and Cav1.2 is abolished by AuF and restored by AD4 (NAC-amide). (a) Representative superimposed $\alpha_1$1.2/β2/α2δ current traces (Cav1.2) in the absence and in the presence of AuF (*left*); Sx1A/Sx1A + AuF as indicated *(middle)* or Sx1A+AuF+AD4 *(right)*. (b) Leak subtracted current-voltage relationships of $\alpha_1$1.2/β2/α2δ expressed either alone (○) or with AuF (□, left); Sx1A/Sx1A + AuF (●/▲, middle) or Sx1A+AuF+AD4 (◀, right). Inward Ca^{2+} currents were evoked from a holding potential of −80 mV to various test potentials in response to 200 ms test pulse at 5 mV increments. (c) G/Gmax values as indicated in b (d) τ activation values as indicated in b. The data points correspond to the mean ± SEM of currents (n = 8–15).

the reaction of Sx1A/biotin-NM (**Fig. 6b**). In cells that subsequent to AuF treatment were incubated with 1 mM N-acetylcysteine amide (AD4), or thioredoxin mimetics (TXM) 100 μM NAc-CysProCys-amide (CB3), or 10 μM NAc-CysGlyProCys-amide (CB4)[28,31], the reactivity to biotin-NM was preserved (**Fig. 6b *lower***).

The Biotin-Switch assay was performed also in oocytes injected with the RFP-Sx1A^{C145A} mutant (**Fig. 6c**). Exposure to AuF yielded a lower level of Sx1A^{C145A} mutant, which was similar to Sx1A. These results indicate that oxidation by AuF is not mediated by the intracellular C145 but rather through the TM Cys residues. Subsequent treatment with the small thiol reducing compounds reversed the AuF effects, as shown by restoration of Sx1A labeling with biotin-NM pulled-down assay.

Consistent with VGCC kinetics being modulated by the oxidation-reduction state of Sx1A as monitored in oocytes, and by the biotin-NM-strep-avidin pull-down of Sx1A, the oxidation by AuF inhibits CA release in chromaffin cells and is reversed by AD4, CB3, and CB4[28] (**Fig. S3**), but not by the non-thiol ascorbic acid (**Fig. S4**). These results highlight a major role for the Sx1A/channel interaction in the redox sensitivity of the release process.

A Chemical approach to test AuF binding to Sx1A transmembrane domain. The binding of AuF-gold atom to Sx1A was used to probe a covalent disulfide linkage of AuF with Sx1A C271 and C272. Towards that end a recombinant His-tagged RFP-Sx1A^{C145A} mutant was expressed in *Xenopus* oocytes (**Fig. 7a**). Oocytes were treated with or without 5 μM AuF for 30 min, and His-tagged RFP-Sx1A^{C145A} was purified from the clear-solubilized membrane fraction by Ni-NTA-agarose beads, shown by western blot analysis (**Fig. 7b**). The presence of gold atoms in the purified samples was detected by atomic absorption using mass spectrometry (**Fig. 7c**). Ni-beads-eluted samples from un-injected or wt Sx1A injected oocytes showed background level of 2215 and 1125 gold counts/sec, respectively (**Fig. 7d**). Samples of un-injected oocytes exposed to AuF, exhibited 58,998 gold counts/sec, accounting for non-specific AuF-adsorption/binding. In contrast, gold atoms count in samples of RFP-Sx1A^{C145A} injected oocytes exposed to AuF, was ~ 3000 fold higher (173,178,500 counts/sec) compared to the non-specific binding, indicating AuF-bound to Sx1A (**Fig. 7d**). This chemical approach established a covalent disulfide bond between AuF and the TM Cys residues of Sx1A.

Discussion

We have used a combination of molecular, biochemical, and physiological approaches to evaluate the impact of the redox state of the two highly conserved Cys residues at the TM of Sx1A on VGCC and synchronous release. These studies consolidate the idea that a signal generated during membrane depolarization and subsequent Ca^{2+} occupancy of the channel selectivity-filter is transmitted to the exocytotic machinery through interaction with Sx1A TM domain (reviews[1,2]). We have tested a plausible model in which synchronous release is triggered within the TM milieu by a two-way intramembrane signaling from the channel pore to the TM segment of Sx1A.

We have previously shown a specific effect of mutating Cys within the TM domain of Sx1A on reconstituted capacitance in oocytes. A major goal of the present study was to bridge the gap between the results in the reconstituted system and what actually transpires in a physiological secretory system. The dominant-negative studies of single and double point mutants of Sx1A combined with the direct oxidation of the TM Cys residues, allowed us to make two basic conclusions. First, there is a mechanistic link between the calcium channel and the transmembrane domain of Sx1A[14,16,19,20] that facilitates transmission of a depolarizing-signal from the channel pore directly to TM Cys residues of Sx1A, resulting in the triggering of release. Second, the TM Cys residues of Sx1A confer redox sensitivity upon the exocytotic process.

We have shown that Sx1A, which is the only excitosome-TM protein, is well poised for capturing a signal initiated at the channel pore within the membrane-bilayer milieu. A direct interaction between the channel and the exocytotic machinery, in which Sx1A acts as a signal transducer, is crucial for facilitating the sub-millisecond synaptic signaling.

Mutating the TM vicinal C271 and C272 to Ala, Ser, or Val disrupted the functional contact of Sx1A with the channel, and abolished the negative modulation of Cav1.2 and Cav2.1 current amplitude. This negative regulation recorded in isolation in the oocytes expression system, was reversed by synaptotagmin and SNAP-25 during the assembly of the excitosome[32]. In contrast, the TM mutations did not alter the interaction of the cytosolic domain of Sx1A with the II-III loop of the VGCC, as demonstrated by an increase in the rate of activation[32].

Over-expression of the Sx1A mutants, Cys271V or Cys272V, lowered total CA secretion (~50%) in adrenal chromaffin cells. These dominant negative results were correlated with a loss of a TM interactive modulation of current amplitude, as demonstrated in voltage-clamped oocytes expressing Sx1A mutants. Most likely,

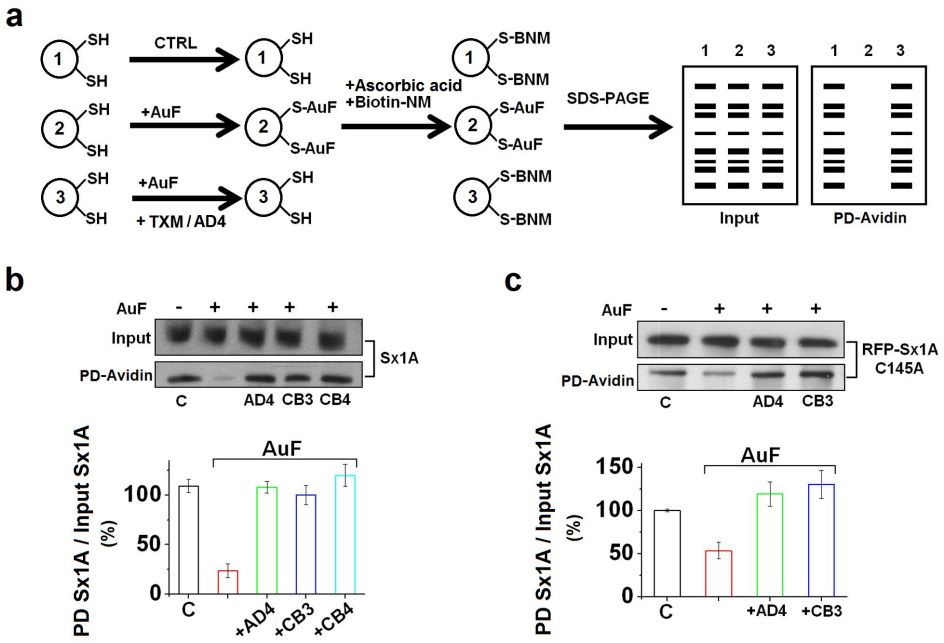

Figure 6 | AuF affects Sx1A availability for Biotin-NM and results in reduced strep-avidin pull down in chromaffin cells and in *Xenopus* oocytes. (a) Schematic depiction of the modified Biotin-NM assay followed by strep-avidin pull-down. (b) Bovine chromaffin cells treated with either AuF or AuF followed by AD4, or CB3 as indicated. Cells were subjected to the modified Biotin-NM assay followed by strep-avidin pull-down and separated on SDS-PAGE *(upper)*. Quantification of Sx1A pull-down with streptavidin *(lower)* (c) *Xenopus* oocytes, injected with cRNA encoding for RFP-Sx1A C145A, were treated with AuF followed by AD4, or CB3 or CB4 (TXM) as indicated. (d) *Xenopus* oocytes, injected with cRNA encoding for RFP-Sx1A C271V/C272V (CC/VV), were treated with or without AuF. All oocytes were lysed and subjected to the modified Biotin-NM assay followed by Strep-avidin pull-down and separation on SDS-PAGE *(upper)*. Quantification of Sx1A pull-down with strep-avidin *(lower)*. The data points correspond to the mean ± SEM (n = 3). Two sample Student's t-test assuming unequal variance was applied and p values were obtained from two tailed test; *$p < 0.05$, **$p < 0.01$, ***$p < 0.001$.

Sx1A TM mutants interfered with signal propagation by loosing contact with the channel. The mutation, which led to improper assembly of the exocytotic unit, resulted in inhibition of secretion.

Moreover, the decrease in the initial rate of secretion strongly suggests that the channel interacts with a mixture of endogenous wt and mutated Sx1A molecules. CA release appears to be less efficient when the mixed clusters of Sx1A assemble with the channel, as opposed to clusters containing only wt Sx1A. These results are consistent with a model in which more than one Sx1A molecule associates with the channel[20]. A cluster of a large number of Sx1A molecules was previously suggested to facilitate exocytosis in PC12 cells[33].

Interestingly, conservation of specific residues within a TM domain of proteins, except for an overall conservation of hydrophobic character, is atypical, unless they serve a functional role[34]. Therefore, we suggest that the critical role of Sx1A C271 and C272 in transducing synchronous release could account for a unique cellular function[35,16,20].

Our data could not be compared to CA release stimulated by photolysis of caged-calcium. Even though, caged calcium by elevating global Ca^{2+} in the cell bypasses the physiological stimulus of membrane depolarization and VGCC activation, it does not fully mimic the physiological triggered fusion event. It induces an abrupt large amperometric signal that corresponds to CA released from many vesicles combined, which cannot be dissected into individual spikes[36].

It is widely accepted that the Cys residues within the hydrophobic milieu of the membrane bilayer are hydrogen-bonded to i-4 backbone carbonyl oxygen[37]. Electrostatic calculations showed that the TM-sulfhydryl groups in a model of phospholamban contribute to the electrostatic potential field of the protein[38].

Disruption of the Sx1A/Cav1.2 interaction by a thiol-oxidizing reagent indicates that Cys271 and C272 in the cell exist in the reduced state. Hence, these Cys residues might contribute to the electrostatic potential field of Sx1A. We validated the engagement of Sx1A TM Cys and the VGCC further by demonstrating that unlike the single cytosolic C145, the reduced state of Sx1A TM is essential for interaction with the channel, and for triggering secretion.

Furthermore, the redox sensitivity of Sx1A/channel interaction, which is abolished by AuF treatment and restored by AD4 or CB3, is in good correlation with the AuF effects on abolishing CA release, and AD4 or CB3 on restoring CA release in chromaffin cells[28] (**Fig. S3; Table SIV**) or insulin release in insulinoma cells[31]. Interestingly, the slow endothelial granule exocytosis that occurs within minutes after stimulation, involves syntaxin 4, an isoform that has no TM Cys residues. Unlike CA release in chromaffin cells the redox sensitivity of endothelial exocytosis depends entirely on intracellular cysteines[39,40].

The impact of the redox state of Cys271 and C272 on the Sx1A/channel interaction was confirmed also biochemically. Using the biotin-NM assay[30,41], the Sx1A sulphydryl groups reacted with biotin-NM under normal cellular conditions, but failed to react in AuF-treated cells. The disulfide bond formed between Sx1A TM Cys and AuF was reduced subsequent to treatment with the thiol reducing reagents, AD4, CB3 or CB4, as demonstrated by restoring the reaction with biotin-NM. This reversible redox behavior of the Sx1A/Cav1.2 interaction is consistent with the oxidizing effect of phenylarsene-oxide and its reversal by 2,3-dimercaptopropanol[16,20].

In non-excitable endothelial cells, lacking Sx1A, inhibition of thrombin-induced release of granules by H_2O_2 was attributed to oxidation of a critical Cys residue of an intracellular redox sensor, the NEM-sensitive factor[42–44].

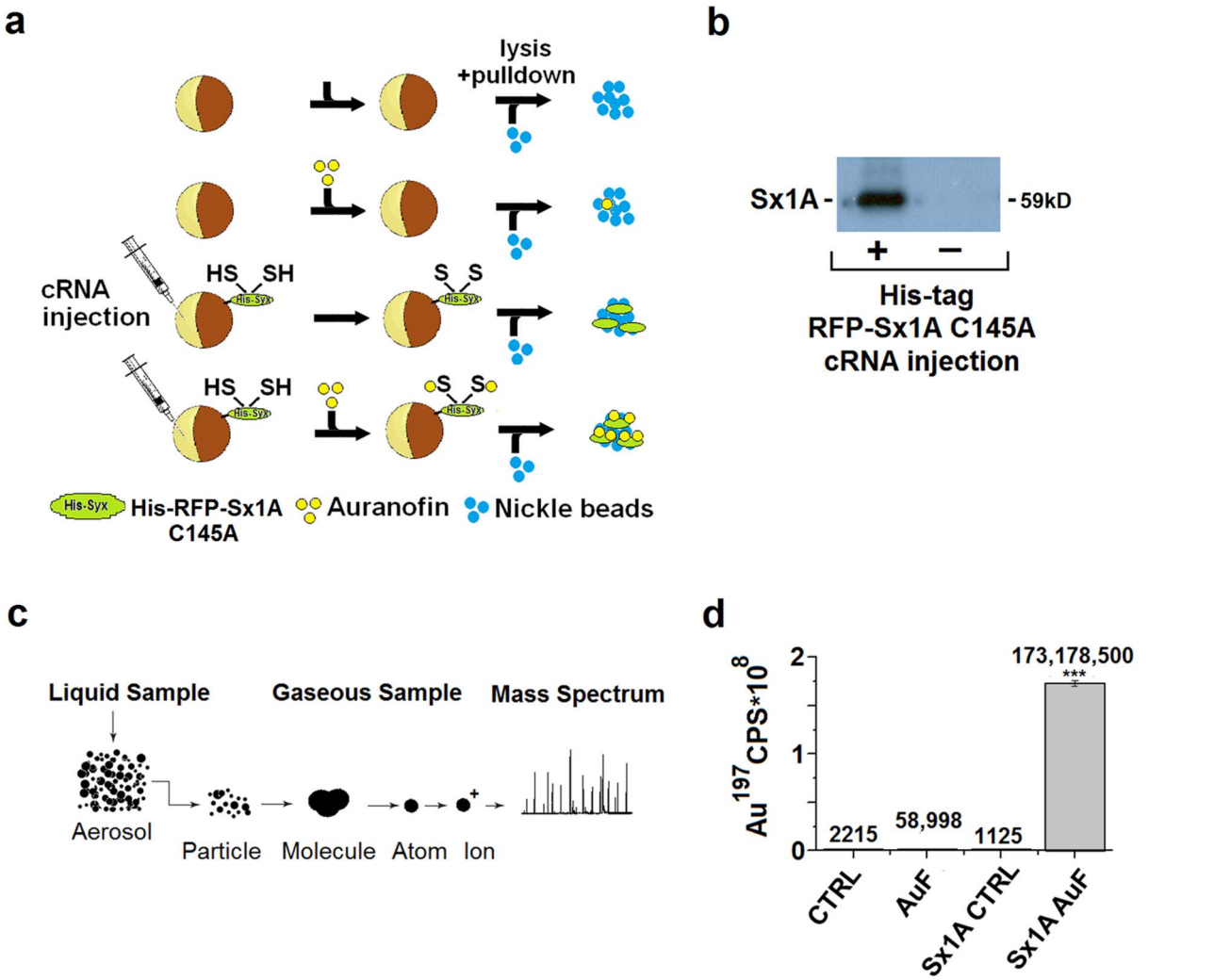

Figure 7 | Sx1A binds AuF detected by gold atoms using mass spectrometry. (a) Schematic depiction of the pull-down assay. His-tag RFP-Sx1A^{C145A} was expressed in *Xenopus* oocytes bound to AuF and pulled-down by Ni^{2+} beads. (b) Western blot analysis of His-tag RFP-Sx1A^{C145A} pulled down with Ni^{2+} beads. (c) Schematic depiction of element detection via mass spectrometry. (d) Gold (Au^{197}) detection (counts per second, CPS) via mass spectrometry of oocytes either injected (Sx1A) or un-injected (Un) with cRNA of His-tag-RFP-Sx1A^{C145A}. Oocytes were treated with AuF as indicated. Lysates were subjected to pull-down as described in a.

Our studies show that the Sx1A^{C145A} mutant has no effect on Cav1.2 kinetics, or on CA secretion, as opposed to nitrosylation of Sx1A^{C145}, which was shown to decrease the rate of exocytosis[45]. In contrast to the unique impact of C271 and C272 on the release process, our results indicate no effect of Sx1A cytosolic C145 on the redox sensitivity of the depolarization-evoked release.

The presence of several Cys residues in TM domains are found across eukaryotes in a wide range of tail-anchored membrane proteins like Sx1A[46]. These Cys modules were proposed to act as an electrostatic switch[47] playing a protective role against various metal ions and other chemical stress stimuli. Perhaps, oxidizing of Sx1A TM Cys, which leads to immediate halt of secretion, denotes resistance to a stress signal, thus full-filling an important cellular function[46].

Forming a disulfide bond between AuF and Sx1A provided a chemical evidence for the reduced state of Sx1A Cys residues. AuF, an organo-gold oxidizing-reagent, known for its thiol reactivity, reacted covalently with the Sx1A TM Cys. The AuF-gold atoms were detected by mass spectrometry in Ni-purified His-tagged Sx1A^{C145A} from AuF-treated oocytes. Gold atoms were not detected in non-injected oocytes, or in Sx1A injected oocytes that were not exposed to AuF.

In summary, our dominant negative experiments and voltage-clamped studies corroborate a dynamic coupling between VGCC and Sx1A. Sx1A C271 and C272 mutants inhibit depolarization-evoked release and disrupt the Sx1A interaction with the channel. The exhibited decrease in the initial rate of secretion by the TM mutants is compatible with the association of more than one Sx1A molecule with the calcium channel. The activated VGCC interacts with the reduced form of TM Cys residues of Sx1A, which is essential for triggering release[1,2,11,14,16]. Oxidizing C271 and C272 inhibits both Sx1A/channel interaction and CA release. The restoration of synchronous release and Sx1A/channel interaction by reversing C271 and C272 oxidation highlight the Sx1A contribution to the redox sensitivity of the exocytotic process. Together, the results support the excitosome model in which a conformation coupling initiated during voltage-perturbation by Ca^{2+}-binding to the pore of the VGCC and prior to permeation, triggers synchronous release of channel-tethered vesicles through dynamic intra-membrane interactions with Sx1A.

Methods

Reagents. The following materials were purchased from Sigma (Jerusalem, Israel), if not otherwise stated: collagenase A, Auranofin (triethylphosphine

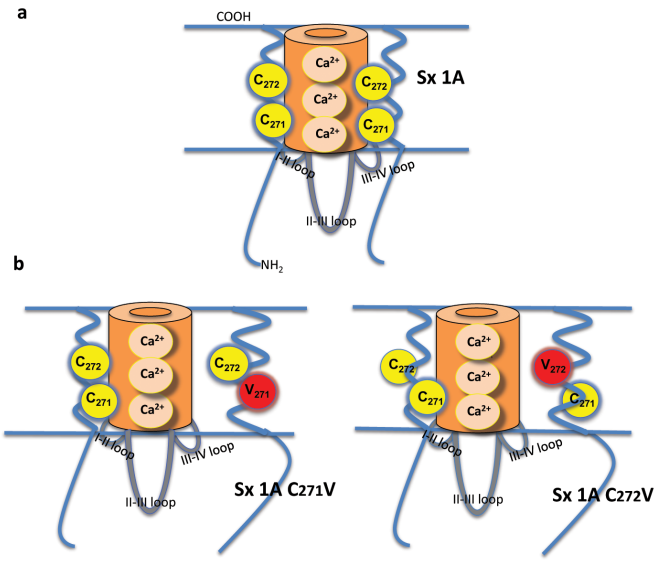

Figure 8 | Schematic presentation of an intra-membrane cross talk between wt Sx1A or Sx1A single mutants with the α_1 subunit of VGCC. (a) Interaction between the calcium channel and Sx1A occurs through the SH group of TM Cys271 and Cys272 (for simplicity only two Sx1A molecules and a single channel are shown). (b) Mutating or oxidizing the Cys residues disrupts the transmembrane interaction between Sx1A and the channel yielding 'inefficient' contact with the channel, and affects evoked release. The cytosolic Sx1A/channel interaction is not affected by the redox state of the Sx1A TM domain cysteines.

(2,3,4,6-tetra-O-acetyl-β-1-D-thiopyranosato-S) gold(I)) AuF, Trx-mimetic peptides, (custom synthesized by Novetide Ltd., Haifa, Israel, and Proimmune, UK) and AD4 (NAC-amide; Novetide), Biotin Maleimide, Strep-avidin Agarose Resin (Thermo Scientific, U.S.A), Tissue culture serum and medium were obtained from Biological Industries (Kibbutz Beit-Haemek, Israel), Vitamin C (Merck, Germany). Adrenal glands were provided by Khaled Zoabe, the Holon Slaughter house.

cDNA constructs. Human $\alpha_1$2.1 (accession # NM_000068) was obtained from T. Snutch. The rat β2A (m80545), β3 (M88751) and rabbit $\alpha_1$1.2 subunit (accession # X15539) were obtained from N. Qin and Dr. L. Birnbaumer (NC, USA). The α2/δ rabbit skeletal (accession # M86621) was from A. Schwartz (OH, USA).

Sx1A (accession #M95734) was obtained from M.L. Bennett. *RFP Syx1A* was prepared by insertion of the Eco47III-HindII RFP monomer fragment into EcoRV site of syntaxin 1A as previously described[20].

The double mutant C271V, C272V of RFP-Sx1A C271V/C271/V) was prepared by the quick-change method (Stratagene, LaJolla, CA) using RFP-Sx1A as a template with the primers- 5′ GGAAGAAGATCATGATCATCATTGTCGTTGTGATT-CTGGGCATCATCATCGCC and 3′ CCTTCTTCTAGTACTAGTAGTAACAG-CAACACTAAGACCCGTAGTAGTAGCGG.

The following mutations were prepared by the same method:

RFP Sx1A$^{CC/SS}$ by using the primers-

Forward 5′GGAAGAAGATCATGATCATCATTTCCTCTGTG3′

Reverse 5′GGTGGAGGCGATGATGATGCCCAGAATCACAG3′

RFP Sx1A$^{CC/AA}$ by using the primers-

5′GGCACGCAGGAAGAAGATCATGATCATCATTGCCGCTGTGATTCTG-GGCATCATCATC3′

5′GATGATGATGCCCAGAATCACAGCGGCAATGATCATGATCTTCTTC-CTGCGTGC3′

The single RFP Sx1A mutants:

RFP Syx1A^{C271V}

5′GGCACGCAGGAAGAAGATCATGATCATCATT**GTCT**GTGTGATTCTG-GGCATCATCATC3′

5′GATGATGATGCCCAGAATCACACA**GAC**AATGATCATGATCTTCTTC-CTGCGTGC3′

RFP Syx1A^{C272V}

5′GGCACGCAGGAAGAAGATCATGATCATCATTTGC**GTT**GTGATTCTG-GGCATCATCATC3′

5′GATGATGATGCCCAGAATCAC**AAC**GCAAATGATCATGATCTTCTTC-CTGCGTGC3′

RFP Syx1A^{C145A} by using the primers-

5′TCAGACTACCGAGAACGCGCCAAAGGGCGCATCCAGAGGCAG3′

5′CTGCCTCTGGATGCGCCCTTTGGCGCGTTCTCGGTAGTCTGA3′

Mutagenesis was performed by PCR followed by Dpn I digest of the product.

The final constructs in Semliki Virus were prepared by a PCR made of the RFP syntaxin coding region of each of the above constructs and ligated to the Semliki Forest Virus vector, pSFV4

Two-electrode voltage-clamp recordings in *Xenopus laevis* oocytes. Stage V and VI oocytes were surgically removed from female *Xenopus* laevis as previously described[17]. Capped polyA cRNAs from linearized cDNA templates encoding rabbit Cav1.2 subunit $\alpha_1$1.2 (5-7 ng), rabbit β_{2b} (2.7 ng), and rabbit $\alpha_2\delta_1$ (5-7 ng) subunits or human Cav2.1 $\alpha_1$2.1 (8.5 ng), rabbit β_3 (1.7 ng), and rabbit $\alpha_2\delta_1$ (5.0 ng) were co-injected into oocytes and whole-cell currents were recorded using the standard two-electrode voltage-clamp configuration in BAPTA-injected oocytes (5 mM) as previously described[17].

Recordings were made in Ca^{2+} solution (mM): 5$Ca(OH)_2$, 50 N-methyl d-glucamine, 1 KOH and 5 HEPES (pH 7.5), titrated to pH 7.5 [$(CH_3)_2SO_4$].

Voltage clamp and data analysis. Inward calcium currents (I_{Ca}) were elicited from a holding potential of -80 mV to various test potentials at 5 mV intervals, by a 200 ms test pulse. Channel kinetics was recorded using the standard two-electrode voltage clamp method[17].

Biotin switch assay. Chromaffin cells/*Xenopus* laevis oocytes were exposed to 5 mM AuF for 30 min then washed and incubated with or without AD4 (1000 mM); CB3 (100 μM) or CB4 (100 μM) for 30 min. Later, cells were harvested with buffer A (2 mM MgAc, 50 mM Tris-Cl, pH 7.5), 1% tween and 1% Ribolock protease inhibitor cocktail (Fermentas/Thermo scientific, USA). The lysates were incubated with 10 mM ascorbic acid for 20 min and later incubated with 4 mM Biotin-NM for 30 min. Excess Biotin-NM was removed via PD MidiTrap G-25 sepharose beads (GE Healthcare, UK). Equal amounts of protein were incubated with strep-avidin beads for 1 hr. Biotinylated proteins were centrifuged at 1200 rpm, and the pellet was washed with buffer A. Strep-avidin-precipitated proteins were eluted with lysis buffer (150 mM Tris–HCl, pH 6.8, 10% glycerol, 0.6% SDS, bromophenol blue) and separated by SDS-PAGE.

Western blot analysis and antibodies. Proteins were loaded onto 10% SDS–PAGE gels. The proteins were then transferred electrophoretically to nitrocellulose transfer membrane (Whatman, Germany). The blots were blocked by incubation for 1 hr at room temperature in TBS-T (25 mM Tris–HCl, pH 7.4, 0.9% NaCl, and 0.02% Tween-20) with 4% skim milk (Difco, Becton–Dickinson, USA). The blots were incubated overnight at 4°C with anti Sx1A (Sigma, Israel) primary antibody, diluted in 5% bovine serum albumin, 0.04% azide in TBS-T. Proteins were detected with anti-rabbit IgG HRP-linked antibody (Cell Signaling Technology, USA).

Bovine chromaffin cell preparation and culture. Bovine adrenal glands were obtained at a local slaughterhouse. The adrenal medulla cells were isolated as described previously[28]. Cells were plated at a density of 5×10^4 cells/cm^2 on glass coverslips placed in 35-mm plates, and cultured in DMEM (Gibco/Invitrogen, USA) supplemented with ITS-X and PenStrep (Sigma, Israel). Cells were incubated at 37°C in 5% CO_2 and used for amperometric recordings 2–4 days after preparation at 23°C.

Amperometric recordings of catecholamine release from bovine chromaffin cells. Amperometry recordings were carried out using 5 μm-thick carbon fiber electrodes, CFE (ALA, Inc., Westbury, NY, USA) and a VA-10 amplifier (NPI-Electronic, Tamm, Germany) held at 800 mV as described previously[28]. Cells were rinsed three times before the experiment and bathed during the recordings in isosmotic physiological solution (149 mM NaCl, 2 mM KCl, 1 mM MgCl2, 2 mM CaCl2, 10 mM glucose, 10 mM HEPES, pH 7.3, at ~23°C). Before the recording, spontaneous release was monitored for a 10 s period for each cell and then recording was initiated. Ten seconds after the recording started, individual cells were stimulated to release by a 10 s application of isosmotic 60 mM KCl (K60) from a ~3 μm tipped micropipette placed 5 μm from the cell. Amperometric currents were sampled at 10 kHz, using Clampex 9.2 (Axon Instruments, USA) and low-pass filtered at 0.2 kHz. Secretion from single vesicles results in amperometric currents represented by spikes. Presentation of a single amperometric event is shown as an amperometric spike and the corresponding foot current[48]. Total secretion was determined by integrating the area underneath the amperometric spike and presented as picocoulombs (pC).

Semliki Forest Virus Infection. Semliki Forest viruses of wt RFP Sx1A, RFP-Sx1A^{C271V}, RFP-Sx1A^{C272V}, RFP-Sx1A^{C145A}, and RFP-Sx1A$^{CC/VV}$ mutants[20] were prepared, and chromaffin cells were infected as described previously[22].

Kinetic parameters of catecholamine release in chromaffin cells. The overall time course of secretion was determined from normalized waiting-time distributions constructed by spike counting[48]. The maximal slopes of the corresponding cumulative spike plots correspond to the initial rates of secretion during the 10- to 30-s of each recording. Total secretion was calculated as the integrated area under the spikes and averaged per cell. The number of spikes per cell was calculated and averaged per cell.

His-tag-RFP-Sx1A^{C145A} Pull-Down Assay. cRNA of His-tag RFP-Sx1A^{C145A} was injected into *Xenopus* oocytes. Three days later, the oocytes were exposed to 5 mM AuF for 30 min, lysed in buffer A (2 mM MgAc, 50 mM Tris-HCl, pH 7.5),

supplemented with 1% Ribolock protease inhibitor cocktail. Lysates were centrifuged at 80 g for 5 min, pellet was discarded, 0.5% Triton was added and supernatant was centrifuged at 18,200 g. Pellet was discarded and supernatant was incubated with Ni-NTA agarose (Qiagen GmbH, Germany) for 1 hr. Samples were washed three times in PBS-0.1% Triton supplemented with 8 M Urea. Elution was done with 0.5 M imidazole.

Mass Spectrometry. Samples generated from the Pull-Down assay of His tag-RFP-Sx1A^{C145A} were centrifuged at 80 g to get rid of residual beads. HNO_3 was added to final concentration of 1% c/v. Mass spectrometry data was obtained via Inductively-Coupled Plasma Mass Spectrometry (Agilent Technologies, UK).

1. Atlas, D. Signaling role of the voltage-gated calcium channel as the molecular on/off-switch of secretion. *Cell Signal* **22**, 1597–1603 (2010).
2. Atlas, D. The Voltage-Gated Calcium Channel Functions as the Molecular Switch of Synaptic Transmission. *Annu Rev Biochem* **82** (2013).
3. Sheng, Z. H., Rettig, J., Takahashi, M. & Catterall, W. A. Identification of a syntaxin-binding site on N-type calcium channels. *Neuron* **13**, 1303–1313 (1994).
4. Wiser, O., Tobi, D., Trus, M. & Atlas, D. Synaptotagmin restores kinetic properties of a syntaxin-associated N-type voltage sensitive calcium channel. *FEBS Lett* **404**, 203–207 (1997).
5. Wiser, O., Bennett, M. K. & Atlas, D. Functional interaction of syntaxin and SNAP-25 with voltage-sensitive L- and N-type Ca^{2+} channels. *EMBO J* **15**, 4100–4110 (1996).
6. Mochida, S., Sheng, Z. H., Baker, C., Kobayashi, H. & Catterall, W. A. Inhibition of neurotransmission by peptides containing the synaptic protein interaction site of N-type Ca^{2+} channels. *Neuron* **17**, 781–788 (1996).
7. Degtiar, V. E., Scheller, R. H. & Tsien, R. W. Syntaxin modulation of slow inactivation of N-type calcium channels. *J Neurosci* **20**, 4355–4367 (2000).
8. Cohen, R. & Atlas, D. R-type voltage-gated Ca(2+) channel interacts with synaptic proteins and recruits synaptotagmin to the plasma membrane of Xenopus oocytes. *Neuroscience* **128**, 831–841 (2004).
9. Bezprozvanny, I., Zhong, P., Scheller, R. H. & Tsien, R. W. Molecular determinants of the functional interaction between syntaxin and N-type Ca^{2+} channel gating. *Proc Natl Acad Sci U S A* **97**, 13943–13948 (2000).
10. Rettig, J. *et al.* Isoform-specific interaction of the alpha1A subunits of brain Ca^{2+} channels with the presynaptic proteins syntaxin and SNAP-25. *Proc Natl Acad Sci U S A* **93**, 7363–7368 (1996).
11. Cohen-Kutner, M., Nachmanni, D. & Atlas, D. CaV2.1 (P/Q channel) interaction with synaptic proteins is essential for depolarization-evoked release. *Channels (Austin)* **4**, 266–277 (2010).
12. Weiss, N. & Zamponi, G. W. Control of low-threshold exocytosis by T-type calcium channels. *Biochim Biophys Acta* (2012).
13. Leung, Y. M., Kwan, E. P., Ng, B., Kang, Y. & Gaisano, H. Y. SNAREing voltage-gated K+ and ATP-sensitive K+ channels: tuning beta-cell excitability with syntaxin-1A and other exocytotic proteins. *Endocr Rev* **28**, 653–663 (2007).
14. Trus, M., Wiser, O., Goodnough, M. C. & Atlas, D. The transmembrane domain of syntaxin 1A negatively regulates voltage-sensitive Ca(2+) channels. *Neuroscience* **104**, 599–607 (2001).
15. Wiser, O., Cohen, R. & Atlas, D. Ionic dependence of Ca^{2+} channel modulation by syntaxin 1A. *Proc Natl Acad Sci U S A* **99**, 3968–3973 (2002).
16. Arien, H., Wiser, O., Arkin, I. T., Leonov, H. & Atlas, D. Syntaxin 1A modulates the voltage-gated L-type calcium channel (Ca(v)1.2) in a cooperative manner. *J Biol Chem* **278**, 29231–29239 (2003).
17. Wiser, O. *et al.* The voltage sensitive Lc-type Ca^{2+} channel is functionally coupled to the exocytotic machinery. *Proc Natl Acad Sci U S A* **96**, 248–253 (1999).
18. Tobi, D., Wiser, O., Trus, M. & Atlas, D. N-type voltage-sensitive calcium channel interacts with syntaxin, synaptotagmin and SNAP-25 in a multiprotein complex. *Receptors Channels* **6**, 89–98 (1998).
19. Cohen, R., Schmitt, B. M. & Atlas, D. Molecular identification and reconstitution of depolarization-induced exocytosis monitored by membrane capacitance. *Biophys J* **89**, 4364–4373 (2005).
20. Cohen, R., Marom, M. & Atlas, D. Depolarization-evoked secretion requires two vicinal transmembrane cysteines of syntaxin 1A. *PLoS One* **2**, e1273 (2007).
21. Lerner, I. *et al.* Ion interaction at the pore of Lc-type Ca^{2+} channel is sufficient to mediate depolarization-induced exocytosis. *J Neurochem* **97**, 116–127 (2006).
22. Hagalili, Y., Bachnoff, N. & Atlas, D. The voltage-gated Ca(2+) channel is the Ca(2+) sensor protein of secretion. *Biochemistry* **47**, 13822–13830 (2008).
23. Wightman, R. M. *et al.* Temporally resolved catecholamine spikes correspond to single vesicle release from individual chromaffin cells. *Proc Natl Acad Sci U S A* **88**, 10754–10758 (1991).
24. Breckenridge, L. J. & Almers, W. Currents through the fusion pore that forms during exocytosis of a secretory vesicle. *Nature* **328**, 814–817 (1987).
25. Snyder, R. M., Mirabelli, C. K. & Crooke, S. T. The cellular pharmacology of auranofin. *Semin Arthritis Rheum* **17**, 71–80 (1987).
26. Offen, D. *et al.* A low molecular weight copper chelator crosses the blood-brain barrier and attenuates experimental autoimmune encephalomyelitis. *J Neurochem* **89**, 1241–1251 (2004).
27. Grinberg, L., Fibach, E., Amer, J. & Atlas, D. N-acetylcysteine amide, a novel cell-permeating thiol, restores cellular glutathione and protects human red blood cells from oxidative stress. *Free Radic Biol Med* **38**, 136–145 (2005).
28. Bachnoff, N., Trus, M. & Atlas, D. Alleviation of oxidative stress by potent and selective thioredoxin-mimetic peptides. *Free Radic Biol Med* **50**, 1355–1367 (2011).
29. Holmgren, A. & Lu, J. Thioredoxin and thioredoxin reductase: current research with special reference to human disease. *Biochem Biophys Res Commun* **396**, 120–124.
30. Jaffrey, S. R., Erdjument-Bromage, H., Ferris, C. D., Tempst, P. & Snyder, S. H. Protein S-nitrosylation: a physiological signal for neuronal nitric oxide. *Nat Cell Biol* **3**, 193–197 (2001).
31. Cohen-Kutner, M. *et al.* Thioredoxin-mimetic peptides (TXM) reverse auranofin induced apoptosis and restore insulin secretion in insulinoma cells. *Biochem Pharmacol* **85**, 977–990 (2013).
32. Atlas, D., Wiser, O. & Trus, M. The voltage-gated Ca^{2+} channel is the Ca^{2+} sensor of fast neurotransmitter release. *Cell Mol Neurobiol* **21**, 717–731 (2001).
33. Barg, S., Knowles, M. K., Chen, X., Midorikawa, M. & Almers, W. Syntaxin clusters assemble reversibly at sites of secretory granules in live cells. *Proc Natl Acad Sci U S A* **107**, 20804–20809 (2010).
34. von Heijne, G. Membrane proteins up for grabs. *Nat Biotechnol* **25**, 646–647 (2007).
35. Trus, M. *et al.* The L-type voltage-gated Ca^{2+} channel is the Ca^{2+} sensor protein of stimulus-secretion coupling in pancreatic beta cells. *Biochemistry* **46**, 14461–14467 (2007).
36. Nagy, G. *et al.* Regulation of releasable vesicle pool sizes by protein kinase A-dependent phosphorylation of SNAP-25. *Neuron* **41**, 417–429 (2004).
37. Arkin, I. T., Russ, W. P., Lebendiker, M. & Schuldiner, S. Determining the secondary structure and orientation of EmrE, a multi-drug transporter, indicates a transmembrane four-helix bundle. *Biochemistry* **35**, 7233–7238 (1996).
38. Arkin, I. T. *et al.* Structure of the transmembrane cysteine residues in phospholamban. *J Membr Biol* **155**, 199–206 (1997).
39. Lowenstein, C. J. & Tsuda, H. N-ethylmaleimide-sensitive factor: a redox sensor in exocytosis. *Biol Chem* **387**, 1377–1383 (2006).
40. Yamakuchi, M. *et al.* Exocytosis of endothelial cells is regulated by N-ethylmaleimide-sensitive factor. *Methods Mol Biol* **440**, 203–215 (2008).
41. Prior, I. A. & Clague, M. J. Detection of thiol modification following generation of reactive nitrogen species: analysis of synaptic vesicle proteins. *Biochim Biophys Acta* **1475**, 281–286 (2000).
42. Matsushita, K. *et al.* Hydrogen peroxide regulation of endothelial exocytosis by inhibition of N-ethylmaleimide sensitive factor. *J Cell Biol* **170**, 73–79 (2005).
43. Matsushita, K. *et al.* Nitric oxide regulates exocytosis by S-nitrosylation of N-ethylmaleimide-sensitive factor. *Cell* **115**, 139–150 (2003).
44. Ito, T., Yamakuchi, M. & Lowenstein, C. J. Thioredoxin increases exocytosis by denitrosylating N-ethylmaleimide-sensitive factor. *J Biol Chem* **286**, 11179–11184.
45. Palmer, Z. J. *et al.* S-nitrosylation of syntaxin 1 at Cys(145) is a regulatory switch controlling Munc18-1 binding. *Biochem J* **413**, 479–491 (2008).
46. Venancio, T. M. & Aravind, L. CYSTM, a novel cysteine-rich transmembrane module with a role in stress tolerance across eukaryotes. *Bioinformatics* **26**, 149–152 (2010).
47. Carugo, O. *et al.* Vicinal disulfide turns. *Protein Eng* **16**, 637–639 (2003).
48. Marom, M., Hagalili, Y., Sebag, A., Tzvier, L. & Atlas, D. Conformational changes induced in voltage-gated calcium channel Cav1.2 by BayK 8644 or FPL64176 modify the kinetics of secretion independently of Ca^{2+} influx. *J Biol Chem* **285**, 6996–7005 (2010).

Acknowledgments

We thank the H. L. Lauterbach Fund (for (DA). O. Tirosh for Mass spectrometry measurements.

Author contributions

N.B. performed the amperometry studies and viral infections. M.C.K. performed the oocytes experiments. M.T. cloned the Sx1A mutants. D.A. wrote the main manuscript text and prepared figure 8. N.B. and M.C.K. prepared figures 1-7. All authors reviewed the manuscript.

Additional information

Supplementary information accompanies this paper at http://www.nature.com/scientificreports

Competing financial interests: The authors declare no competing financial interests.

How to cite this article: Bachnoff, N., Cohen-Kutner, M., Trus, M. & Atlas, D. Intra-membrane Signaling Between the Voltage-Gated Ca^{2+}-Channel and Cysteine Residues of Syntaxin 1A Coordinates Synchronous Release. *Sci. Rep.* **3**, 1620; DOI:10.1038/srep01620 (2013).